

# Senior Seminar : The Bispectrum as a Quantifier of Dust Contamination in the Cosmic Microwave Background

■ Vishal Kasliwal

## Abstract

Theoretical models predict that the Cosmic Microwave Background (CMB), a remnant of the BigBang, is Gaussian in nature. An assessment of this prediction is complicated by large quantities of interstellar dust, primarily within our galaxy, thought to possess a highly non-Gaussian signature. It is important to confirm the theoretical model. The bispectrum is evaluated as a good quantifier of non-Gaussianity in the CMB maps. IDL routines have been written to calculate the bispectrum of data-sets from the Wilkinsons Microwave Anisotropy Probe (WMAP) mission to map the CMB. The question that shall be addressed is whether dust contamination, in both large and small amounts, significantly affects the bispectrum.

## Introduction

The Cosmic Microwave Background (CMB) is a remnant of the BigBang and consists of a continuous background at a mean temperature of 2.73K. The light from the CMB comes from the surface of 'last scattering', when photons last interacted with matter. Until roughly three thousand years after the BigBang, matter in the Universe existed in the ionized form. Light constantly interacted with this ionized matter, and so the Universe was opaque to light. At the 'time of recombination', when neutral atoms started to form, light could travel freely through the Universe. The temperature of the CMB is not a constant function of position, but shows local variations of the order of  $10^{-5}$ K. This anisotropy of the CMB is supposed to have been caused by quantum-mechanical processes occurring momentarily after the BigBang, before the time of recombination. Theoretical models predict that these anisotropies should be Gaussian in nature, meaning that if a small square patch of the sky is considered, the coefficients of the Fourier transform of the patch should be independently drawn from a Gaussian distribution. Attempts to measure the CMB using satellites such as WMAP (NASA) to verify the theoretical predictions have been complicated by the presence of low temperature dust and gas within our galaxy. Low temperature dust and gas radiate strongly in the microwave part of the electromagnetic spectrum, creating a foreground contaminant.

## Preliminaries

A statistic, known as the bispectrum, was chosen to quantify the amount of dust contamination in CMB maps. Computer code was then written in the IDL data analysis software to implement the bispectrum and all associated tools.

The CMB map consist of a map of the temperature fluctuation of the CMB from the mean of 2.73K. This map is defined on the surface of the celestial sphere, and so, is not flat. However, the sheer amount of data available makes it impossible to compute statistics on the whole sphere at once, particularly since Fourier transforms are not defined on curved surfaces. Therefore, the technique used is to consider small, square patches of the full map at a time, and treat them as flat, permitting a computation of the Fourier transform. It must be kept in mind that the discontinuity of a map at the edges of the map introduces errors in the computation of the Fourier transform, and a technique known as data-windowing must be used to circumvent this problem. For a square patch of the sky  $[0,a] \times [0,a]$  where  $a$  is the number of pixels on the map, the data-window is a function,  $f(x,y)$  defined on the region  $[0,a] \times [0,a]$  such that the function drops to 0 on the boundary of the region. Multiplying this data-window by the map then causes the map to be continuous at the edges of the map, resulting in the correct Fourier transform. The data-window function chosen was the Haan data-window. A one-dimensional plot of the Haan data-window is shown in Fig 1.

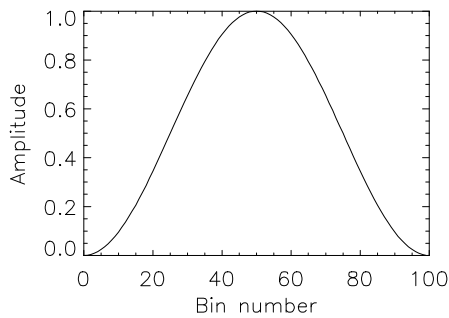


Fig 1 : The Haan Data Window

A commonly tool used when talking about the CMB is the powerspectrum of the CMB. Given a small square patch of the CMB map, the powerspectrum of the patch is defined as the two point correlation function of the Fourier transform of the patch. The powerspectrum is an indicator of the strength of features of various scales in the patch under consideration. If  $M(x,y)$  represents the temperature fluctuation of the CMB at pixel  $(x,y)$  on the patch, let  $\tilde{M}(k_x, k_y)$  be the Fourier transform of the patch at wavenumbers  $k_x, k_y$ . The pair  $(k_x, k_y)$  represents a vector in the Fourier transform of the patch, therefore let  $l = \|(k_x, k_y)\|$  be the length of the vector  $(k_x, k_y)$ . The powerspectrum is then given by

$$\mathcal{P}(l_1, l_2) = \langle \tilde{M}(l_1) \tilde{M}(l_2) \rangle$$

where the brackets denote an ensemble average. It should be noted that the powerspectrum cannot be used to quantify dust contamination as it is possible for two maps, one with dust contamination, and the other without, to share the same powerspectrum. Fig 2 shows a plot of the powerspectrum of the CMB.

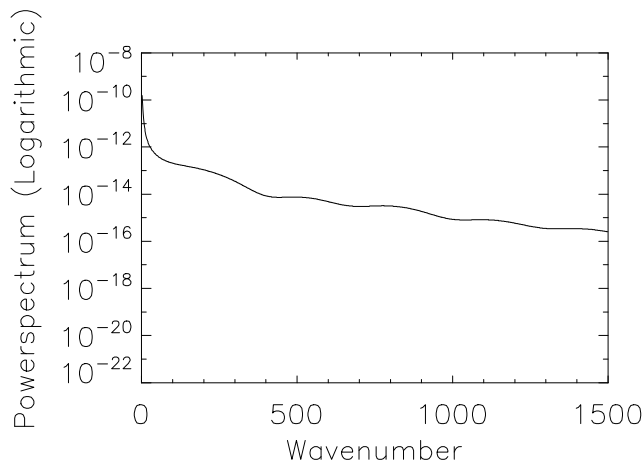


Fig 2 : The Powerspectrum of the CMB

Gaussian maps were artificially generated using IDL code. Recall that a map is Gaussian if the coefficients of the Fourier transform of the map are drawn independently from a Gaussian distribution. Therefore, IDL's random number generator was used to implement `makemap.pro`, a tool that, given a powerspectrum function, generates square maps of a given pixel size and angular resolution. Real data from satellites such as WMAP is limited by the angular resolution of the sensors on board the satellite. The effect of having finite angular resolution is to lower the powerspectrum at high wavenumbers, corresponding to a loss of features at low wavelengths. Therefore, the function `smoothmap.pro` was written to emulate the finite angular resolution of real data by lowering the angular resolution of the artificial maps generated by `makemap.pro`. Satellite electronics introduce artificial noise into the data-set. Therefore a tool called `addnoise.pro` was written to add Gaussian random noise to a patch generated by `makemap.pro` to emulate real data-sets.

D. Finkbeiner, D. Schlegel and M. Davis have generated a map of galactic dust at CMB temperatures in their paper [4], and have published this map on the internet. A data-set exhibiting pure dust contamination was obtained from the website of the authors, and the tool `dustpatch.pro` was written to extract random square patches of a given pixel size and angular swath from the full sky data-set. The data-set generated by Drs. Finkbeiner, Schlegel and Davis is a data-set of pure dust. It is believed that real data obtained from satellites exhibits a Gaussian background with a low level of actual dust contamination. Therefore, a tool, `combinemap.pro`, was implemented to superimpose a specified level of dust contamination on a Gaussian background. Examples of Gaussian, dust and combined maps are shown in Fig 3, 4 and 5.

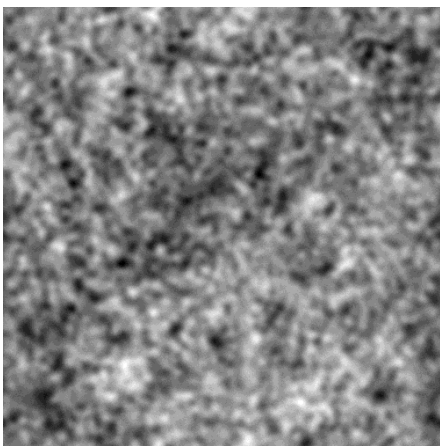


Fig 3 : A Gaussian map

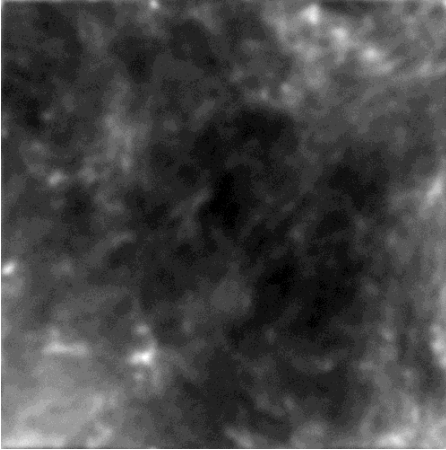


Fig 4 : A dust patch

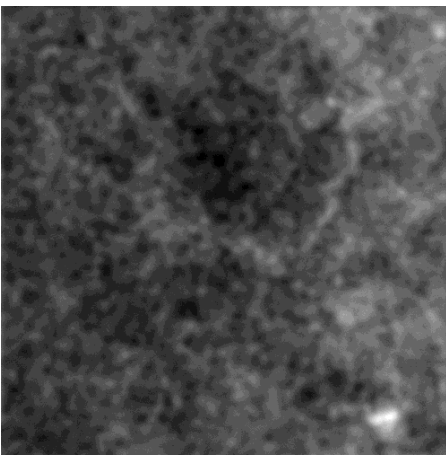


Fig 5 : A combined map

## The Bispectrum

The bispectrum is defined as the three-point correlation function of the Fourier transform of a map. Therefore, it is a function of three variables. To intuitively understand the bispectrum, visualize the Fourier transform of a map,  $M(x,y)$ , as another map,  $\tilde{M}(k_x, k_y)$ , of the same pixel dimensions since the original data-set is discrete. The co-ordinates of the map correspond to the various  $k_x$  and  $k_y$  values in the Fourier transform of the map. Given a point  $q = (k_x, k_y)$  on the Fourier transform of the map i.e.  $\tilde{M}$ , the distance of the point from the origin, i.e. the length of the vector  $(k_x, k_y)$  is  $l = \|(k_x, k_y)\|$ , just as in the case of the powerspectrum. Three such points,  $q_1, q_2$  and  $q_3$ , define a triangle in Fourier space. The bispectrum as a function of the distances of the three points from the origin is an average of the products of the value of the Fourier transform of the map at each vertex over all triangles of identical geometry for all possible triangles i.e. an ensemble average over all possible triangle geometries.

$$B(l_1, l_2, l_3) = \langle \tilde{M}(l_1)\tilde{M}(l_2)\tilde{M}(l_3) \rangle$$

The mathematical properties of Fourier transforms imposes certain restrictions on the possible geometries that may be considered when evaluating the bispectrum. The three sides of the triangle must necessarily obey the triangle in-equality. Additionally, the vector sum of the three points forming the triangle must add up to the zero vector. If  $q_1 = (k_{x1}, k_{y1})$ ,  $q_2 = (k_{x2}, k_{y2})$  and  $q_3 = (k_{x3}, k_{y3})$ , then

$$q_1 + q_2 + q_3 = 0$$

which leads to two scalar equations,

$$k_{x1} + k_{x2} + k_{x3} = 0$$

$$k_{y1} + k_{y2} + k_{y3} = 0$$

If this condition is not met, then the bispectrum will evaluate to zero for the given set of three lengths. This condition has a very useful practical application. It allows the algorithm for computing the bispectrum to be run over just two random points instead of all three, since the condition automatically fixes the third point once the first two are specified, saving on computation time.

Interesting sub-cases of the bispectrum exist. One particularly interesting sub-case is the linear bispectrum. The linear bispectrum is the bispectrum for all degenerate triangles in the Fourier transform of the original map i.e. triangles formed by points lying on a straight line in Fourier space. The bispectrum then effectively reduces to a function of two variables since the combination of the linearity condition and the vector sum condition fixes the third point on a line through the origin. Shown in Fig 6 and Fig 7 are plots of the linear bispectrum of a Gaussian map and a dust map.

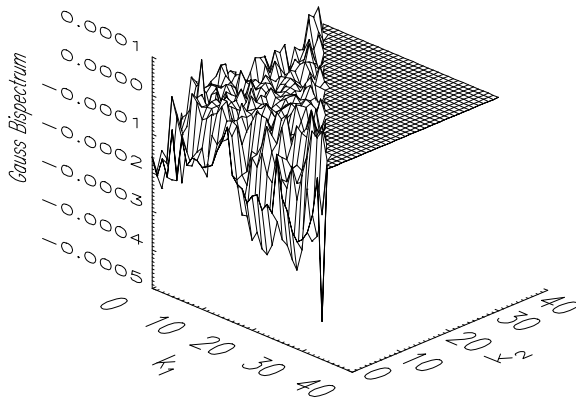


Fig 6 : The linear Gaussian bispec-

trum

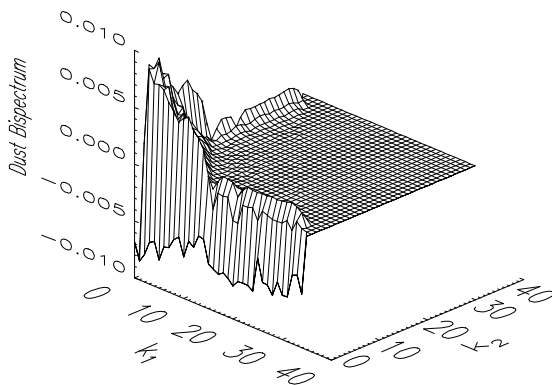


Fig 7 : The linear dust bispectrum

## Analysis Techniques

The bispectrum is a function of three variables, and the linear bispectrum is effectively a function of two variables. To aid in the analysis of the bispectra data, the bispectrum was flattened by simply rearranging the data into a linear column, i.e. a function of one variable, and another data-set was created to keep track of where individual entries in the bispectrum came from in three-dimensional space.

Bispectra from Gaussian maps were compared to bispectra from dust and combined maps by carrying out a principal-component analysis on the Gaussian and dust bispectra to obtain directions in the bispectra along which dust bispectra differed most from Gaussian bispectra. Let there be  $n$ -entries in the flattened bispectrum. The principal component analysis then gives  $n$  principal vectors of  $n$ -dimensions each. A plot of the first principal vector is shown in Fig 8.

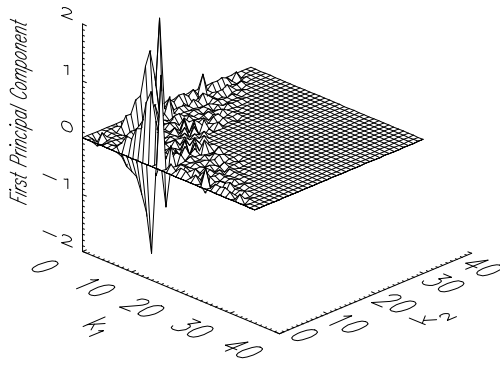


Fig 8 : The first principal component vector

A test map may be either a dust map or a combined map with a certain level of dust contamination. A set of test maps consists of a set of either all pure dust maps or all combined maps, all with the same level of dust contamination. Suppose  $m$  Gaussian and  $m$  test maps were analyzed. If  $E_i$  denotes one such principal vector where  $i \in \mathbb{Z}_n$ , and  $B_j$  denotes the bispectrum of the  $j$ -th map where  $j \in \mathbb{Z}_m$  then the matrix  $A_{ij}$  was calculated where

$$A_{ij} = E_i B_j$$

Since this matrix was calculated for both Gaussian and test maps, let  $G_{ij}$  be the matrix  $A_{ij}$  for Gaussian maps, and  $t_{ij}$  be the matrix  $A_{ij}$  for test maps. Let  $\mu_i$  be the mean of the matrix  $G_{ij}$  over all  $m$  maps and  $\sigma_i$  be the standard-deviation of the matrix  $G_{ij}$  over all  $m$  maps, i.e.

$$\mu_i = \frac{1}{m} \sum_{j=1}^m G_{ij}$$

$$\sigma_i = \sqrt{\sum_{j=1}^m \frac{(G_{ij} - \mu_i)^2}{m}}$$

A  $\chi$ -square statistic may be carried out. Define the  $\chi$ -squares of the Gaussian maps,  $\chi_j^G$  where the G-superscript indicates Gaussian  $\chi$ -squares, as

$$\chi_j^G = \sum_{i=0}^n \frac{(G_{ij} - \mu_i)^2}{\sigma_i^2}$$

Test  $\chi$ -squares,  $\chi_j^t$  where the superscript t denotes test  $\chi$ -squares, may be identically defined as

$$\chi_j^t = \sum_{i=0}^n \frac{(t_i - \mu_i)^2}{\sigma_i^2}$$

Consider the q-th percentile of the Gaussian  $\chi$ -squares. Let  $\chi_q^G$  be the  $\chi$ -square number corresponding to the q-th percentile of the Gaussian  $\chi$ -squares. The set S may be defined as

$$S = \{ \chi_j^t \mid \chi_j^t \geq \chi_q^G \}$$

S is the set of  $\chi$ -squares for all test maps such that their  $\chi$ -square is higher than the q-th percentile of the Gaussian  $\chi$ -squares. The cardinality of the set S,  $\text{Card}(S)$ , gives the number of such test maps. The percentage of test maps such that their  $\chi$ -square value belongs to S is the power of the test, P.

$$P = 100 \times \frac{\text{Card}(S)}{m}$$

## Results

An analysis of the bispectrum was carried out for three types of test maps - pure dust maps, combined maps with 50% dust combination, and combined map with 25% dust contamination against Gaussian maps generated using makemap.pro. The number of maps considered in each case was 14600 maps. Each map was smoothed to an angular resolution of 0.3 degree/pixel to closely match the performance characteristics of the WMAP satellite. Although the WMAP satellite sensors add approximately 10% of artificial noise contamination, for the time being no noise was added to our data-sets. The bispectrum was then calculated for each map, and an analysis of the resulting bispectrum data carried out as outlined above.

It is to be expected that up to a certain point, considering more principal component vectors would increase the power of the test, P. After a certain point, the principal component vectors carry information about how the two given data-sets are similar to each other, rather than how they differ. Therefore, the power of the test was calculated with various, increasing, numbers of principal component vectors considered. Plots are shown below for the power of the test, P against the number of principal component vectors, 'nkeep', considered.

First, consider the results for pure dust maps in Fig 9.

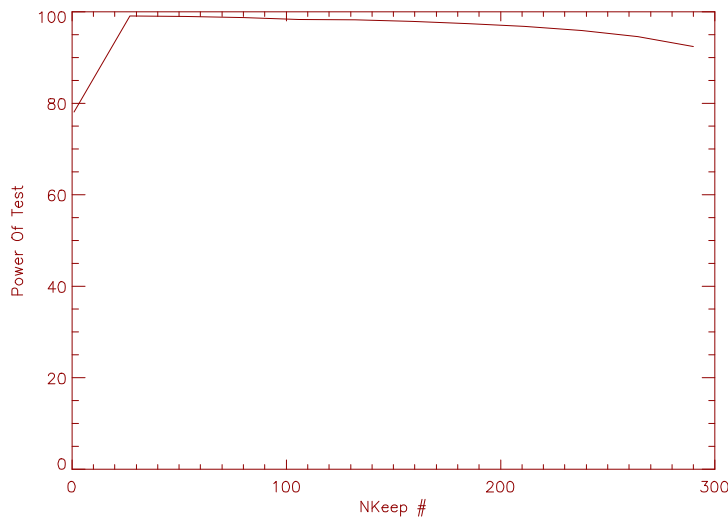


Fig 9 : Power of the Test v/s nkeep for pure dust maps

As can be seen from the graph, the bispectrum is a good detector of pure dust, with P reaching 100% for 30 principal

component vectors.

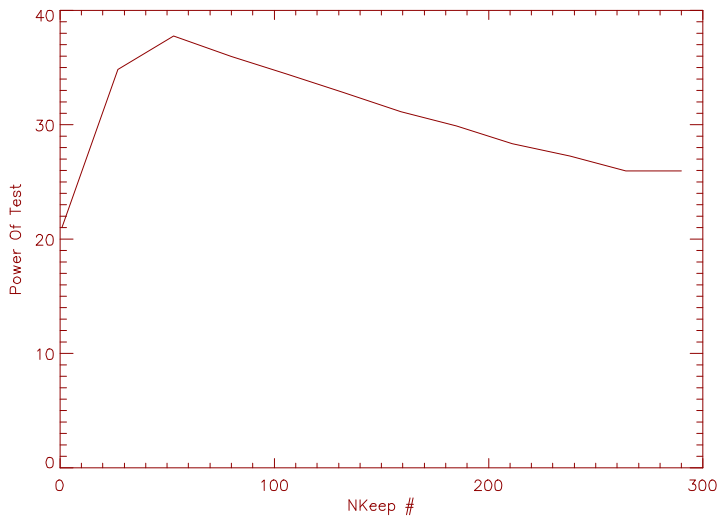


Fig 10 : Power of the Test v/s nkeep for combined maps with 50% dust contamination

As can be seen from the graph in Fig 10, the power of the test drops considerably for combined maps with 50% dust with a maximum of 38% occurring at 50 principal component vectors retained.

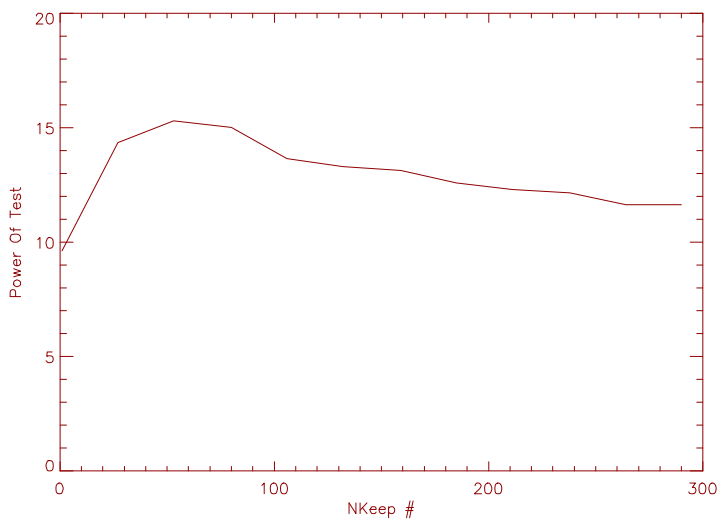


Fig 11 : Power of the Test v/s nkeep for combined maps with 25% dust contamination

From the graph in Fig 11, it may be seen that the power of the test drops still further for combined maps with 25% dust with a maximum of 15% occurring at 50 principal component vectors retained.

This indicates that while the bispectrum may be a good indicator of pure dust, it is not good at detecting low levels of dust contamination.

## Conclusion

Even though the bispectrum is not a powerful quantifier of dust contamination in the CMB, its insensitivity to dust contamination indicates that it may be a good quantifier of true CMB non-Gaussianity. Several theoretical models predict a non-Gaussian CMB, in which case, if the bispectrum proves to be a good at distinguishing Gaussian CMBs from the suggested non-Gaussian CMBs, then the insensitivity of the bispectrum to dust contamination will become an asset.

## References

[1] "First Year Wilkinson Microwave Anisotropy Probe (WMAP) Observations: Preliminary Maps and Basic Results"  
Bennett et al., *Astrophys.J.Suppl.* 148 (2003) 1

[2] "First Year Wilkinson Microwave Anisotropy Probe (WMAP) Observations: Foreground Emission"  
Bennett et al., *Astrophys.J.Suppl.* 148 (2003) 97

[3] "First Year Wilkinson Microwave Anisotropy Probe (WMAP) Observations: Tests of Gaussianity"  
Komatsu et al., *Astrophys.J.Suppl.* 148 (2003) 119-134

[4] "Maps of Dust IR Emission for Use in Estimation of Reddening and CMBR Foregrounds"  
D. J. Schlegel, **D. P. Finkbeiner**, and Marc Davis, [ApJ, 500, 525](#) (20 June, 1998), also [astro-ph/9710327](#)

This work was supported by NSF grant 0233969 and by a Cottrell Award from the Research Corporation